ASCA and ROSAT Observations of NRAO 140 and IX Per

T. J. Turner

I. M. George, G. M. Madejski

S. Kitamoto, T. Suzuki

Laboratory for High Energy
Astrophysics

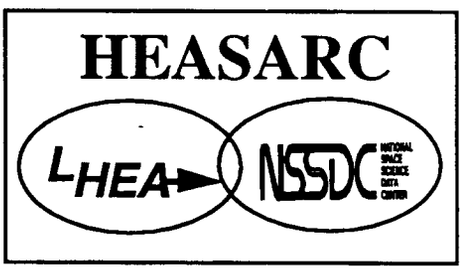

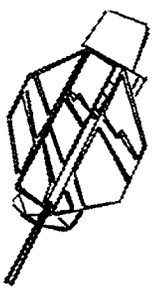

ROSAT
Science
Data
Center

High Energy Astrophysics Science
Archive Research Center

NASA Goddard Space Flight Center
Greenbelt, MD 20771

ASCA AND *ROSAT* OBSERVATIONS OF NRAO 140 AND IX Per

T.J. Turner [1,2], I.M. George [1,2], G.M. Madejski [1,2], S. Kitamoto [3] and T. Suzuki [3]

Received _____; accepted Dec 8 1994

Accepted for publication in *The Astrophysical Journal*

[1]Laboratory for High Energy Astrophysics, NASA/Goddard Space Flight Center, Greenbelt, MD 20771

[2]Universities Space Research Association

[3]Department of Earth and Space Science, Faculty of Science, Osaka University, 1-1, Machikaneyama-cho, Toyonaka, Osaka, 560, Japan

ABSTRACT

We report the results from observations of NRAO 140 carried out in the X–ray band using *ROSAT* and *ASCA* in 1992 and 1994. We find the source to be absorbed by an effective hydrogen column density of $\sim 3 \times 10^{21}$ atoms cm^{-2} during both epochs, consistent with the combined atomic and molecular column inferred from radio measurements along this line-of-sight through the Perseus cloud complex. We compare these results with previous X–ray absorption measurements and briefly comment upon the origin of the excess absorption which has been seen towards this source.

We find the *ASCA* spectrum of NRAO 140 is well described by a power law of energy index $\alpha = 0.73 \pm 0.03$, and also yields the tightest constraint to date on Fe K-shell emission, with 90% confidence upper limits of 38 and 31 eV for a narrow line at a rest-frame energy of 6.4 and 6.7 keV respectively. This, along with a lack of hardening towards higher energies, suggests that either NRAO 140 is devoid of cold reprocessing material, the reprocessing material has a geometry in which the imprinted features are weak, and/or the X–ray emission is relativistically beamed towards us.

We also report the detection of a serendipitous source in both the *ASCA* GIS and *ROSAT* fields-of-view. We identify this source as the binary star system IX Per, and find its spectrum to be well fitted by a two-temperature Raymond-Smith plasma.

Subject headings: ISM: structure — quasars: individual (NRAO 140) — radio sources: individual (NRAO 140) — X–rays: quasars — X–rays: stars — stars: individual (IX Per)

1. Introduction

The extremely high luminosities exhibited by some quasars may indicate an extreme accretion rate, or a high degree of relativistic beaming. If the former is true, then the highest luminosity quasars are the most X–ray luminous objects in the universe and the observed properties imply that they are fueled by central black holes of mass $> 10^8 M_\odot$. If the latter is true, and relativistic beaming is a characteristic property of bright quasars, then the identification of the parent population is important not just for understanding AGN, but also has implications for the cosmic X–ray background.

NRAO 140, a flat radio spectrum (FRS) quasar at a redshift of z = 1.258, is one of the brightest and most luminous known X–ray quasars with an apparent luminosity $L_{2-10\mathrm{keV}} \sim 10^{47}$ ergs s^{-1} (Marscher 1979). NRAO 140 is also a bright, core-dominated radio source exhibiting superluminal motion with an apparent separation velocity of $4.8h^{-1}c$ between the radio components and the core (for $\mathrm{q}_o = 0.5$ and $\mathrm{H}_o = 100h$ km s^{-1} Mpc^{-1}), and thus its radio emission is most likely to be relativistically beamed (Marscher 1988a). Beamed radio emission is further supported by the lack of copious synchrotron self-Compton emission in the optical–X-ray regime. Even though there is no *direct* evidence, the correlation between the factor 2 increase in both radio and X–ray fluxes (cf. Marscher 1988a) also suggests the X–ray emission from this source may be beamed towards us.

The line-of-sight to NRAO 140 lies close to the Galactic plane ($b = -18.8°$), and behind the outer edge of a giant molecular cloud in Perseus (Ungerechts & Thaddeus 1987; Bania, Marscher, and Barvanis 1991). The total (atomic and molecular) neutral hydrogen column density from 21cm and ^{12}CO measurements is estimated to be $\sim 3 \times 10^{21}$ atoms cm^{-2} (see Section 4.1). Interestingly, previous X–ray observations (Petre et al. 1984; Marscher 1988a; Turner et al. 1991) have shown variable absorption along the line-of-sight to NRAO 140, corresponding to effective hydrogen column densities in the range ~ 3–20×10^{21}

atoms cm^{-2} (assuming cosmic abundances and photoelectric cross-sections), and in one (potentially unreliable) measurement the column was as low as $\lesssim 0.1 \times 10^{21}$ atoms cm^{-2}. These variations in the X–ray column density are likely to be due to the passage of absorbing material across the line-of-sight. Marscher (1988b; see also Fiedler et al. 1994) has suggested that this matter may be a clump of scale size $\lesssim 1$ AU within the Perseus molecular cloud. However, a component intrinsic to NRAO 140 is also a possibility.

Here we present *ROSAT* and *ASCA* observations of NRAO 140 carried out during 1992 and 1994. Details of the observations and data reduction are given in Section 2, and the results of the spectral analysis in Section 3. In Section 4, we discuss our X-ray absorption measurements in the context of those obtained previously in the radio and X-ray bands, along with the implications of the tight upper limit on Fe K-shell emission we obtain from NRAO 140. We also present an X–ray spectrum of the RS CVn star IX Per, which is detected as a serendipitous source in the field-of-view.

2. Data Reduction

2.1. *ROSAT* Data

ROSAT observed NRAO 140 on 1992 August 8, with the Position Sensitive Proportional Counter (PSPC; Pfeffermann et al. 1986) in the focal plane. The 4039 sec exposure indicated that there are no strong X–ray sources close enough to NRAO 140 to cause any confusion in the analysis of the *ASCA* data. Two serendipitous sources are evident to the south-west of NRAO 140, one faint, $\sim 14.5'$ away, and another, brighter object, $\sim 25'$ away. The positions obtained from the *ROSAT* data are summarized in Table 1. The J2000 radio position of NRAO 140 (from the VLA calibrator catalog) is $03^h36^m30.11^s, +32^\circ18'29.3''$ (consistent to within 2 arcsec of the optical position). In an attempt to identify the serendipitous

sources, we conducted a cone search on the relevant available databases. IX Per (also known as HD 22124) lies at an optical position of (J2000) $03^h35^m01.1^s, +32°01'04''$, and as there are no other known candidates, we identify the bright X–ray source as IX Per. No known counterpart was found for the faint source, and we designate it RX J033537+3208.6 following the standard naming convention. The offset between the optical and X–ray positions of NRAO 140 and IX Per are approximately the same size and in the same sense, indicating that the discrepancy is an aspect solution positional error of $\sim 15''$ which dominates over the statistical error (which for on-axis PSPC sources should be only on the order of 5″; Hasinger et al. 1992, 1994). The derived X–ray positions of the three sources are also given in Table 1.

The *ROSAT* PSPC exposure was sufficient to allow a crude determination of the spectra of NRAO 140 and IX Per. We extracted the PHA data using circles, centered on their X–ray positions, of 2.5′ radius (for NRAO 140) and 5′ (for IX Per; a larger radius was needed since the source is off-axis, where the point-spread function of the telescope is degraded). The background for NRAO 140 was extracted from a ring centered on the source, with the inner radius of 5′, and the outer radius of 10′, while for IX Per, we used a region of 5′ at the same offset angle. No significant source variability was evident in the PSPC light curve of NRAO 140. The spectral analysis of both NRAO 140 and IX Per is presented in Section 4.

2.2. *ASCA* Data

NRAO 140 was observed by *ASCA* for $\sim$ 40 ksec over the period 1994 February 1-3. As described in Tanaka, Inoue & Holt (1994), *ASCA* has two Solid State Imaging Spectrometers (SIS, Burke et al. 1991) each consisting of 4 CCD chips, and 2 Gas Imaging Spectrometers (GIS, Ohashi et al. 1991). The observation of NRAO 140 was carried out

(see Section 4.1). Interestingly, previous X–ray observations (Petre et al. 1984; Marscher 1988a; Turner et al. 1991) have shown variable absorption along the line-of-sight to NRAO 140, corresponding to effective hydrogen column densities in the range $\sim 3-20 \times 10^{21}$

using 1 CCD chip exposed on each SIS, and the data were accumulated in both faint and bright telemetry modes. As NRAO 140 is a relatively faint source in the SIS CCDs, the superior resolution available in faint mode data could not be utilized, and the faint mode data were combined with bright mode data for the analysis. SIS grades 0,2,3 and 4 were used in the analysis. Data were rejected during the passage of the spacecraft through or within 60 seconds of the South Atlantic Anomaly and within 100 seconds following the satellite crossing a day/night orbit boundary. Data were selected when the angle from the Earth's limb was greater than 13° during orbit day and greater than 5° (SIS0) or 10° (SIS1, GIS2, GIS3) during orbit night. Only data taken during passage through regions with geomagnetic rigidity > 7 GeV/c were accepted. After these screening criteria had been applied, we extracted a light curve for each instrument, and manually removed time periods of data dropout or spikes due to high background.

Application of these screening criteria gave an effective exposure time of $\sim$ 30 ksec. Images were extracted from the screened and cleaned data from all instruments, and region descriptors were defined for extracting light curves and spectra. For the two SIS instruments, we used a 3′ circle centered on NRAO 140 with the background taken at the edge of the same CCD chip. For the two GIS instruments, we used 6′ radius extraction cells centered on NRAO 140, with the background taken in a source-free region of the GIS. IX Per was observed at the edge of GIS3, falling partially on the ring of bright background. A spectrum was extracted, performing background subtraction using data from a region of similarly high background. As there is a small ($\sim$ 1 arcmin) pointing offset between the ASCA instruments, IX Per did not fall within the field of view of GIS2.

No significant source variability is evident in the ASCA light curves of NRAO 140. In the case of IX Per, the source was close enough to the edge of the GIS3 field of view that the apparent variability of the count rate (< 30 %) could easily be due to some variable fraction of the source counts falling off the detector, given a spacecraft jitter $\sim 1'$. We

extracted mean spectra for the observation from all four instruments for NRAO 140, and from GIS3 for IX Per.

3. Results

Although the *ROSAT* data were accumulated much earlier than the *ASCA* observation, comparison of the source fluxes at 2 keV indicated that NRAO 140 was at approximately the same flux state in the *ROSAT* and *ASCA* observations (within the nominal flux calibration uncertainties of $\sim$ 10%). Occultation and vignetting corrections were made to the observed flux of IX Per and again this indicated consistent flux states in the *ROSAT* and *ASCA* observations (the flux errors for IX Per were $\sim$ 25% due to its partial occultation by the rib in the PSPC data and its position on the edge of the GIS). The *ROSAT* and *ASCA* spectra were fitted first separately, but then also simultaneously for both NRAO 140 and IX Per. Nonetheless, to allow for possible flux calibration errors and source flux variability, we allowed the relative normalization between the *ROSAT* and *ASCA* spectra to be a free parameter in the fits presented below.

RX J033537.6+3208.6 did not yield enough counts in either the *ROSAT* or *ASCA* observations for a meaningful spectral analysis to be performed.

3.1. NRAO 140

We fitted the *ROSAT* data alone to a power law model (defined such that the flux density $S_\nu \propto \nu^{-\alpha}$) absorbed by an effective neutral hydorgen column, N_H, with abundances and cross-sections as given by Morrison & McCammon (1983). First, assuming the absorbing column density to be entirely local ($z = 0$), we obtain a good fit with $\alpha = 1.33^{+0.95}_{-0.82}$, $N_H = 3.88^{+1.86}_{-1.54} \times 10^{21}$ atoms cm^{-2} and $\chi^2 = 20$ for 18 degrees of freedom,

dof. (90% confidence regions for one interesting parameter, equivalent to $\chi^2_{min} + 2.7$, are quoted throughout.) The corresponding 0.5–2 keV (absorbed) model flux is 2.6×10^{-12} ergs cm^{-2} s^{-1}, and the fit results summarized in Table 2. Simultaneously fitting the data from the four *ASCA* instruments to the same model spectrum, tying the fit parameters together but allowing the relative normalizations of the 4 datasets to vary, we found best–fit values of $\alpha = 0.73 \pm 0.03$, $N_H = 2.99 \pm 0.21 \times 10^{21}$ atoms cm^{-2} and $\chi^2/dof = 708/716$. The 0.5–2 keV flux in this case is 2.7×10^{-12} ergs cm^{-2} s^{-1}, confirming (within the calibration errors of both instruments) no flux change between the *ROSAT* and *ASCA* observation epochs. (We note here that we used the SIS instruments to derive the flux, as, at the time of writing, the absolute flux calibration of the SIS instruments is superior to that of the GIS instruments.) Fitting the four *ASCA* instruments simultaneously with the *ROSAT* data, we find a solution consistent with that performed with the *ASCA* data alone: $\alpha = 0.73 \pm 0.03$, $N_H = 2.97 \pm 0.20 \times 10^{21}$ atoms cm^{-2}, with $\chi^2/dof = 730/736$. The data, model and residuals are shown for this fit in Figure 1.

In addition to these simple models, we fit the data with an absorber whose redshift was allowed to vary between 0 and 1.258 (the redshift of the NRAO 140). No value of redshift gave a significantly better fit than $z = 0$. This demonstrated that there was no statistically preferred location for the absorber as an intervening extragalactic system, or as a column intrinsic to NRAO 140.

Any Fe K-shell line emission in NRAO 140 (emitted in the 6.4–6.7 keV range) would be observed in the 2.8–3.0 keV regime, where the SIS and GIS effective areas and energy resolutions are high. We detected no significant Fe K-shell line emission, with 90% confidence upper limits on equivalent width of 38 eV and 31 eV for a narrow line emitted at 6.4 or 6.7 keV respectively. The implications of this result are further discussed in §4.

3.2. IX Per

IX Per is an RS CVn binary (Drake, Simon & Linsky 1989) with one star of the spectral type F2III-V, and the spectral type of its companion unknown. The system is an ellipsoidal variable, with an orbital period of ~1.33 days and a photometric period of 0.663 days with a Heliocentric Julian Date of primary minimum 2429146.901 The V-band magnitude of the system ranges from 0.02 to 6.66.

The source was first detected in X–rays by the Imaging Proportional Counter (IPC) onboard the *Einstein Observatory* and designated IPC033154+3150 with an IPC count rate of 0.067 ± 0.009 count s^{-1}. Subsequently, it was also detected serendipitously by the *EXOSAT* Channel Multiplier Array (CMA), with a count rate of 0.030 ± 0.002 count s^{-1} when the thin Lexan filter was in the field-of-view. The combined *ROSAT* and *ASCA* data yielded a corrected mean flux of 3.1×10^{-12} erg cm^{-2} s^{-1} in the 0.5–4 keV band. Assuming a distance of 63 pc (Drake, Simon & Linsky 1992), we estimate a 0.5–4 keV luminosity of 1.4×10^{30} erg/sec (±25%).

The background–subtracted GIS3 data indicate that IX Per was detected out to an energy of ~ 4 keV, and the *ROSAT* and *ASCA* data indicate the presence of strong line emission. We found that a single temperature Raymond–Smith plasma model (Raymond & Smith 1977) was inadequate to describe the combined *ROSAT + ASCA* data. However, a good fit was obtained to a two temperature model, absorbed by a single column, with $kT_1 = 0.20^{+0.06}_{-0.03}$ keV and $kT_2 = 1.04^{+0.09}_{-0.08}$ keV, normalized in the ratio 1:2, with $\chi^2/dof = 40/37$. We found no evidence for absorption along the line-of-sight to IX Per, with an upper limit of $N_{\rm H} < 4 \times 10^{19}$ atoms cm^{-2} at 90% confidence, consistent with its location in the solar neighborhood. Due to the serendipitous positioning of IX Per on the edge of the GIS, and close to the PSPC rib, neither dataset was suitable for X–ray timing analysis.

4. Discussion

4.1. Absorption towards NRAO 140

The *ROSAT* and *ASCA* observations presented here have shown an X-ray absorption column of $N_H \sim 3 \times 10^{21}$ atoms cm^{-2} along the line-of-sight to NRAO 140. The neutral, atomic hydrogen density towards NRAO 140, from 21 cm observations has been measured to be $N_{HI} = 1.4 \times 10^{21}$ atoms cm^{-2} (Elvis, Lockman & Wilkes, 1989; using the NRAO 140ft dish, with a 21 arcmin beam) and $N_{HI} = 9 \times 10^{20}$ atoms cm^{-2} (Kuchar & Bania, 1990; using the 305m Arecibo telescope, 4 arcmin beam). The effective hydrogen column density due to molecular gas, from ^{12}CO measurements is $N_{H2} = 1.7 \times 10^{21}$ atoms cm^{-2} (Bania, Marscher & Barvainis; 1991). Thus, from radio observations, the total effective column of neutral hydrogen along the line-of-sight to NRAO 140 is in the range $\sim$ 2.6 – 3.1 $\times 10^{21}$ atoms cm^{-2}, in good agreement with the X-ray results presented here (as may be expected since the molecular content is measured using C and O, the elements responsible for the absorption in the soft X–ray band). Therefore, a comparison of the columns indicated by X-ray and radio measurements makes a compelling argument for the absorber measured in the *ROSAT* and *ASCA* X–ray observations to be Galactic in origin, and dominated by the Perseus molecular cloud. We note that Steidel & Sargent (1992) report weak Mg II absorption features, indicating an absorption line system along the line-of-sight to NRAO 140 at redshift z = 0.9532. However this system is unlikely to be an important contributor to the total X–ray absorbing column reported here.

As can be seen from Table 2, some of the earlier X-ray observations of NRAO 140 showed an X-ray absorption column significantly different to $N_H \sim 3 \times 10^{21}$ atoms cm^{-2}. This is not an artifact of variable contamination by IX Per. While IX Per may have contaminated the *Ginga* and *EXOSAT* spectra of NRAO 140, all of the other X–ray

observations detailed in Table 2 were made using instruments with imaging capability better than 5 arcmin (or having a small field of view) allowing distinction between the two sources. The 1979 March Solid State Spectrometer (SSS) and Monitor Proportional Counter (MPC) data suggest an exceptionally low column. However, this observation is potentially the least reliable of all the NRAO 140 X-ray observations, as water-ice contamination affected some early SSS observations. In addition, we consider the total column density inferred from this observation to be unreasonably low for a source observed at such a low Galactic latitude. In contrast, the 1979 August SSS+MPC and 1980 Feb Imaging Proportional Counter (IPC) and High Resolution Imager (HRI) observations of NRAO 140 both show a large excess over the column observed at the present epoch (by a factor ~ 5). It has been suggested that such excess absorption is consistent with a Galactic origin. Marscher (1988b; see also Bania et al. 1991) has suggested that the Perseus cloud is probably clumpy, and that the variations in excess absorption could arise as a result of the proper motion of the Perseus complex due to Solar motion, Earth orbital motion and differential Galactic rotation changing the line-of-sight to NRAO 140 relative to clouds on an AU size scale. Bania et al. argue that, given the change of absorption of at least 6×10^{21} atoms cm^{-2}, and size of the cloud on the order of 1 AU, the density in the cloud must be more than a few $\times 10^{7}$ atoms cm^{-3}.

Such an explanation for the column variations is further supported by the recent work of Fiedler et al. (1994) who show strong evidence for very structured Galactic material towards NRAO 140. In their study of the so-called "extreme scattering events", possibly responsible for the apparent variability of distant quasars at decimeter radio frequencies, the authors identify structure in the foreground to NRAO 140 in both infrared and 21 cm bands. Specifically Fiedler et al. point out that the IRAS image of this region shows a shell-like structure $\sim 1.2°$ in diameter (first noted by Pauls and Schwartz 1989), which appears to be embedded in the Perseus cloud complex, associated with a nova or supernova explosion. Kinematic studies and the obvious morphology suggest that this is a very active

region, and thus it seems plausible that the X–ray column variations may be associated with this cloud complex. IX Per, at 67 pc, shows very little absorption, thus the excess absorption has to be farther than IX Per, consistent with the Perseus cloud explanation. However, we note from Table 2 that no significant change in absorption is detected between the observations by *EXOSAT* (obtained in 1985 January) and *ASCA* (obtained in 1994 February), suggesting that a particularly large or dense cloud/shell may have blocked the line-of-sight during late 1979–1980, but that NRAO 140 is now observed through a less dense, more uniform part of the Perseus complex. We note NRAO 140 is not unique in its proximity to small-scale structures in our Galaxy. Marscher, Moore and Bania (1993) find variations in formaldehyde (H_2CO) absorption line profiles in molecular clouds towards both NRAO 150 and 3C 111, indicating AU-scale structures may also exist along those lines-of-sight.

Nevertheless, an absorbing system intrinsic to NRAO 140 cannot be discounted based on the data accumulated to date. Indeed, NRAO 140 would not be the only high redshift radio-loud quasar with intrinsic absorption (see Wilkes et al. 1992; Stocke et al. 1992; Madejski 1994), however it would certainly be the only one which has shown significant variability in the absorbing column density.

Further pseudo-contemporaneous observations at 21 cm, ^{12}CO and X–ray wavelengths offer the best chance of determining whether the column variations observed are Galactic or intrinsic to NRAO 140.

4.2. X–ray emission from NRAO 140

In the "Compton-reflection" models widely cited as applicable to Seyfert-1s (Lightman & White 1988; George & Fabian 1991; Matt, Perola & Piro 1991) the underlying,"primary" continuum of active galaxies is assumed to be a power-law with an energy index $\alpha \sim 0.9$,

modified by reprocessing by large amounts of optically thick material in the vicinity of the active nucleus (e.g. see Nandra & Pounds 1994). At rest-frame energies $\gtrsim$2 keV, the most prominent signatures of reprocessing are the Fe K-shell emission and absorption in the 6.4–9.5 keV band, and flattening of the observed spectrum $\gtrsim$ 10 keV due to the "Compton Hump". The strengths of these features is a strong function of the geometry of the reprocessing material, and the characteristics of the primary, illuminating source.

We detect no such signatures in the *ASCA* spectrum of NRAO 140, which in the source-frame extends from 1–25 keV. We find upper limits on any Fe Kα line emission of $\lesssim$ 38 eV and 31 eV at 90% confidence for the source-frame energies of 6.4 keV (FeI) and 6.7 keV (FeXXV) respectively. We also find no evidence for any spectral hardening due to a Compton hump, which might be expected to be visible above an (observer-frame) energy of $\gtrsim$ 4.4 keV. Assuming the popular disk-like geometry for any reprocessing material and an isotropic source of primary radiation, as discussed in George & Fabian (1991), then these constraints are consistent with a disk subtending 2π sterad from the primary source observed at an inclination angle $\gtrsim 80°$, or a smaller disk observed face-on, but subtending $\lesssim \pi/2$ sterad. Alternatively, if the reprocessing occurs in a distribution of optically thick clouds surrounding the primary source (Nandra & George 1994), then the constraints imply a covering faction $\lesssim$30%. In both cases these limits can be relaxed if the implied luminosity per solid angle of the primary radiation source is higher along our line-of-sight than towards any circumnuclear material. Clearly the resultant swamping of any features due to reprocessing is most dramatic if the primary source (or any other continuum source), is relativistically beamed towards us. Given the strong evidence for relativistic beaming of the radio emission, it is possible that the X–rays are also beamed, as has been suggested for other AGN including FRSs (e.g. Worrall & Wilkes 1990).

Williams et al. (1992) have shown that radio-loud quasars in general appear to have weaker Fe K-shell emission lines than Seyfert galaxies. Indeed the absence of these lines

has been proposed as a probe of the beamed nature of X–ray emission in AGN (Yaqoob et al. 1993). Unfortunately, the data collected so far (primarily by *Ginga*) are sparse, and the results are somewhat inconclusive. The spectral index, $\alpha = 0.73 \pm 0.03$, obtained from the *ASCA* observation of NRA0 140 is nearly identical to $\alpha = 0.72 \pm 0.11$ measured in the *Ginga* data (Ohashi et al. 1992), and similar to that in 3C 279 (Makino et al. 1989) and PKS 1502+106 (George et al. 1994). This spectrum is consistent with synchrotron self-Compton models in which the X–ray emission is produced from Compton upscattering of soft photons by relativistic electrons. In a number of AGN this emission component is sometimes observed to extend all the way to GeV energies. The *EGRET* 2σ upper limit on the flux >100 MeV from NRAO 140 is 1×10^{-7} photons cm^{-2} s^{-1} (Fichtel et al. 1994).

5. Summary

Based upon *ROSAT* and *ASCA* observations carried out in 1992 and 1994 we have found that the effective hydrogen column density along the line-of-sight to NRAO 140 is $\sim 3 \times 10^{21}$ atoms cm^{-2}. Such a value is consistent with the (atomic plus molecular) column inferred from radio measurements in this direction towards the Perseus cloud complex. We are unable to determine the redshift of the absorber from the X-ray data, but the X–ray absorption observed at these epochs is entirely consistent with the radio measurements of gas in the Perseus cloud complex. Historically, a higher degree of X–ray absorption has been observed towards NRAO 140, but it remains unclear whether that "excess" absorption is intrinsic to NRAO 140 or is related to sub-structure in the Perseus cloud complex.

We obtain the tightest constraint to date on Fe K line emission in NRAO 140, with 90% confidence upper limits of 38 and 31 eV for a narrow line at a rest-frame energy of 6.4 and 6.7 keV respectively. This absence of Fe Kα line as well as the absence of spectral hardening above the energy of the Fe K-shell edge argues that either the object is devoid of

cold reprocessing material, the reprocessing material has a geometry in which the imprinted features are weak, and/or the X–ray emission is beamed.

The serendipitously observed RS CVn system, IX Per, was found to be unabsorbed with a soft spectrum adequately modelled by a two-temperature Raymond–Smith plasma.

Acknowledgements:

The authors wish to thank Alan Marscher, Richard Mushotzky, Steve Drake, Mike Corcoran, Steve Snowden, Keith Arnaud for useful discussions, and an anoymous referee whose comments greatly improved the final paper. We acknowledge the financial support of USRA (TJT, IMG, GMM). This research was performed using XSELECT (version 1.0h), and made use of data obtained through the High Energy Astrophysics Science Archive Research Center Online Service, provided by the NASA/Goddard Space Flight Center, and the NASA/IPAC Extragalactic Database (NED) operated by the Jet Propulsion Laboratory, Caltech, under contract with NASA.

6. References

Bania, T. M., Marscher, A. P., & Barvanis, R. 1991, AJ, 101, 6

Burke, B. E., Mountain, R. W., Harrison, D. C. Bautz, M. W., Doty, J. P., Ricker, G. R., & Daniels, P. J. 1991, IEEE Trans., ED-38, 1069

Drake, S. A., Simon, T., & Linsky, J. L., 1989, ApJ Supp, 71, 905

Drake, S. A., Simon, T., & Linsky, J. L. 1992, ApJ Supp, 82, 311

Elvis, M., Lockman, F. J., & Wilkes, B. 1989, AJ, 97, 777

Fiedler, R., Pauls, K., Johnston, K. J., & Dennison, B. 1994, ApJ, 430, 595

Fichtel, C. et al. 1994, ApJ Supp, 90, 917

George, I. M., & Fabian, A. C. 1991, MNRAS, 249, 352

George, I. M., Nandra, K., Turner, T. J., & Celotti, A. 1994, ApJ L, 436, L59.

Hasinger, G., Turner, T. J., George, I. M., & Boese, G. 1992, Legacy 2, 77

Hasinger, G., Boese, G., Predehl, P., Turner, T. J., Yusaf, R., George, I. M., & Rohrbach, G., 1994, Legacy 4, 40

Kuchar, T.A. & Bania, T.M. 1990, ApJ, 352, 192

Lightman, A. P., & White, T. 1988, ApJ, 335, 57

Madejski, G. M. 1994, ApJ, 432, 554

Marscher, A. 1979, ApJ, 228, 27

Marscher, A. 1988a, ApJ, 334, 552

Marscher, A. 1988b, in "The Impact of VLBI on Astrophysics and Geophysics", by the

IAU, eds M.J.Reid and J.M. Moran, 35

Marscher, A., Moore, E. M., & Bania, T. M. 1993, ApJ, 419, L101

Makino, F., et al. 1989, ApJ, 347, L9

Matt, G., Perola, & G. C. Piro, L. 1991, A&A, 247, 25M

Morrison, R, & McCammon, D. 1983, ApJ, 270, 119

Nandra, K., & George, I. M., 1994, MNRAS, 267, 974

Nandra, K., & Pounds, K. A., 1994, MNRAS, 268, 405

Ohashi, T., Makishima, K., Ishida M., Tsuru T., Tashiro M., Mihara T., Kohmura, Y., & Inoue H., 1991, Proc. SPIE 1549, 9.

Ohashi, T., Tashiro, M., Makishima, K., Makino, F., Turner, M. J. L., & Williams, O. R. 1992, ApJ, 398, 87

Pauls, T., and Schwartz, P.R. 1989, in Lecture Notes in Physics, 331, The Physics and Chemistry of Interstellar Molecular Clouds, ed. G. Winnewisserr & J.T.Armstrong (Berlin:Springer), 225.

Petre, R., Mushotzky, R.F., Krolik, J.H., Holt, S.S., 1984, ApJ, 280, 499

Pfeffermann, E., et al. 1986, Proc. SPIE, 733, 519

Raymond, J. C., & Smith, B. W. 1977, ApJ Supp, 35, 419

Steidel, C. C., & Sargent, W. L. W. 1992, ApJ Supp, 80, 1

Stocke, J. T., Wurtz, R., Wang, Q., Elston, R., & Januzzi, B. 1992, ApJ, 333, L5

Tanaka, Y., Inoue, H., & Holt, S. S. 1994, PASJ, 46, L37

Turner, T. J., Weaver, K., Mushotzky, R. F., Holt, S., & Madejski, G. 1991, ApJ, 381, 85

Ungerechts, H, & Thaddeus, P. 1987, ApJS, 63, 645

Wilkes, B. J., Elvis, M., Tananbaum, H., McDowell, J. C., & Lawrence, A. 1992, ApJ, 393, L1

Williams, O. R., et al. 1992, ApJ, 389, 157

Worrall, D. M., & Wilkes, B.J. 1990, ApJ, 360, 396

Yaqoob, T., McKernan, B., Done, C., Serlemitsos, P. J., & Weaver, K. A. 1993, ApJ, 416, L5

Table 1: Sources in the field-of-view of NRAO 140 detected by the *ROSAT* PSPC

Source Name	*ROSAT* Positions (J2000)					Count Rates	
	Measured		Derived[a]		Error	PSPC	SIS0
	RA	dec	RA	dec	(")	($\times 10^{-3}$ ct s^{-1})	($\times 10^{-3}$ ct s^{-1})
NRAO 140	03 36 29.3	+32 18 42	03 36 30.11	+32 18 29.3	*b*	227 ± 8	226 ± 3
RX J033537+3208.6	03 35 36.4	+32 08 52	03 35 37.2	+32 08 40	10	13 ± 2	24 ± 1
IX Per	03 35 00.9	+32 01 16	03 35 01.7	+32 01 04	6	363 ± 10	12 ± 2

Notes to Table 1:

[a] After correction of PSPC aspect solution (see text)

[b] No error, field corrected to the radio position of NRAO 140.

Table 2: X–ray Spectra of NRAO 140

Instrument	Date	α	Norm[a]	N_H^b	χ^2/d.o.f.	Ref[c]
Einstein SSS+MPC	1979 Mar	1.37 ± 0.15	5.5	$0 < 0.13$	137/89	P84, T91
		$0.73f$	1.8	$0 < 0.06$	152/90	†
Einstein SSS+MPC	1979 Aug	$1.21\ ^{+0.57}_{-0.40}$	4.0	$16.75^{+10.38}_{-4.92}$	99/89	T91
		$0.73f$	1.5	$11.94^{+2.66}_{-2.31}$	103/89	†
Einstein IPC+HRI	1980 Feb	2.85	0.32	19^{+10}_{-6}	6.0/8	M88
		$0.7f$	0.39	$7.7^{+5.3}_{-2.7}$	9.4/9	M88
EXOSAT ME	1985 Jan	1.60 ± 0.14	0.78	$2.96^{+1.32}_{-0.91}$	280/278	M88
Ginga LAC	1989 Feb	0.72 ± 0.11	0.32	< 12.26	25.2/25	O92
ROSAT PSPC	1992 Aug	$1.33^{+0.95}_{-0.82}$	2.0	$3.88^{+0.95}_{-0.82}$	20/18	†
		$0.73f$	0.92	$2.78^{+0.43}_{-0.38}$	21/18	†
ASCA SIS/GIS	1994 Feb	0.73 ± 0.03	0.87	2.99 ± 0.21	708/716	†
ASCA+ROSAT	—	0.73 ± 0.03	0.85	2.97 ± 0.20	730/736	†

Notes to Table 2:

[a] Unabsorbed flux at 1 keV (rest-frame) in units of 10^{-2} photon cm^{-2} s^{-1} keV^{-1}. Error on the normalization is about 10%

[b] Effective neutral hydrogen column density at z=0, in units of 10^{21} atom cm^{-2}.

[c] References: P84, Petre et al. (1984); M88, Marscher et al. (1988a); T91, Turner et al. (1991); O92, Ohashi et al. (1992); †, this work

Errors are at 90% confidence for one interesting parameter

f denotes the parameter was fixed at the given value during the fit

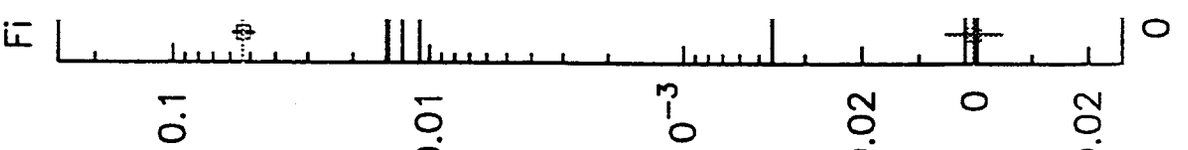

Figure Captions

Figure 1

Top Panel: The *ROSAT* PSPC and *ASCA* SIS0+SIS1+GIS2+GIS3 counts data versus a power-law model absorbed by the Galactic column plus an excess absorber at $z = 0$. The PSPC data are marked with squares. The *ASCA* data indicate there is no significant Fe K-shell emission (which is expected between 2.83 keV and 2.97 keV in the observer's frame). Bottom Panel: Data minus model residuals.

Figure 1

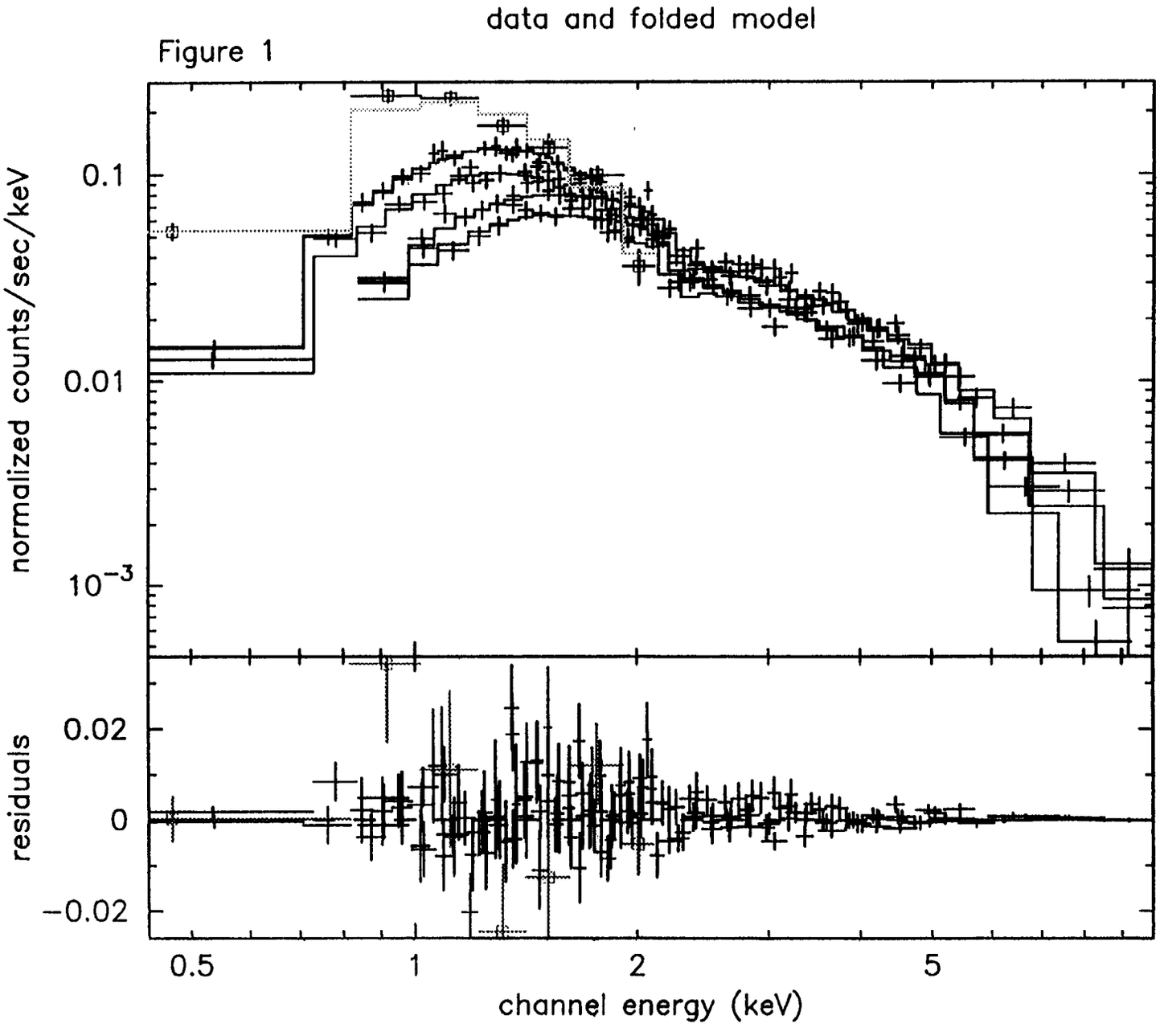
data and folded model
normalized counts/sec/keV
0.1
0.01
10^{-3}
residuals
0.02
0
−0.02
0.5
1
2
5
channel energy (keV)